

Chapter 6

Defective Surfaces of CeO₂

6.1 Introduction

From the literature overview in Chapter 1 it was clear that the presence of oxygen vacancies and Ce³⁺ ions at the surface play a crucial role in the promoter/catalyst properties of CeO₂. Hence, in the present chapter we examine the behaviour of neutral polaron - vacancy clusters at some of the important faces in CeO₂. The study is an initial attempt to build on the models developed for perfect surfaces and apply them to defective surfaces.

6.2 Methodology

6.2.1 Simulation Technique

The calculations were carried out using the MARVIN code, which uses periodic boundary conditions, thus a defect cluster will be repeated throughout space and

Interaction	A(eV)	$\rho(\text{\AA}^{-1})$	C(eV\AA ⁶)	Shell Parameters		
				k(eV\AA ⁻²)	Y(e)	
$O^{2-} - O^{2-}$	9547.92	0.2192	32.00	O^{2-}	9.3	-2.04
$Ce^{4+} - O^{2-}$	1809.68	0.3547	20.40	Ce^{4+}	177.84	-0.20
$Ce^{3+} - O^{2-}$	1629.85	0.3606	2.09	Ce^{3+}	177.84	-0.20

Table 6.1: Short range interactions

must be charge neutral. In the previous chapter the surface energy and attachment energies were studied. However, in the present chapter such quantities are not useful. Instead we refer to the total energy of the block, this will enable us to compare the energetics associated with different defect configurations.

6.2.2 Potential Parameters

The potential parameters are shown in Table 6.1, the $Ce^{4+} - O^{2-}$ interaction is potential 1 from the previous chapter. The $Ce^{3+} - O^{2-}$ was derived using the empiricism techniques discussed in Chapter 2, as little or no experimental data is known on Ce_2O_3 . In addition, for this reason, the shell parameters for Ce^{3+} are identical to those of Ce^{4+} . Although this results in a Ce^{3+} ion which is less polarisable than it should be, the effects of a harder ion are more predictable than one which is too polarisable.

6.3 Neutral defect clusters on the surfaces of CeO_2

6.3.1 The (200) surface

The initial defect studies were carried out on the (200) surface as this face is present if ceria is grown non-stoichiometrically. In addition, the alternate cation - anion layers

on the surface makes the creation of defect clusters simpler.

A number of different defect configurations were examined, and can be classified into two categories. The first is where the vacancy is above the polarons and on the surface, the oxygen vacancy being created on one of the dipole neutralising defect positions (A in Figure 6.1). The second category is where vacancies are placed below the surface plane (B - E in Figure 6.1). In the former category only one unique defect configuration exists, all other possible configurations are symmetrically equivalent. There are four possible arrangements when the vacancy is placed below the surface, as a result of the two ways of orientating the dipole neutralising defects.

Table 6.2 lists the energies of the defects. Configuration A has the lowest unrelaxed energy, and upon relaxation shows very little change in structure. Configurations B-E have much higher unrelaxed energies than configuration A, on relaxation some of these configurations have the same energy as configuration A. These lower energy defect structures are those configurations which can rearrange to allow the vacancy onto the surface and form relaxed structures identical to configuration A. The higher energy structures are simply those that are unable to rearrange to this configuration. Thus we can conclude that on the present surface the preferred position for the oxygen vacancy is to be at the surface. This seems to be in agreement with the work of Sayle *et al.* [27], who showed that oxygen vacancies have a lower formation energy on the surface than in the bulk.

6.3.2 The (111) surface

Using the results from the (200) surface for subsequent faces, only those configurations where the vacancies are at the surface were considered. For the (111) plane two such

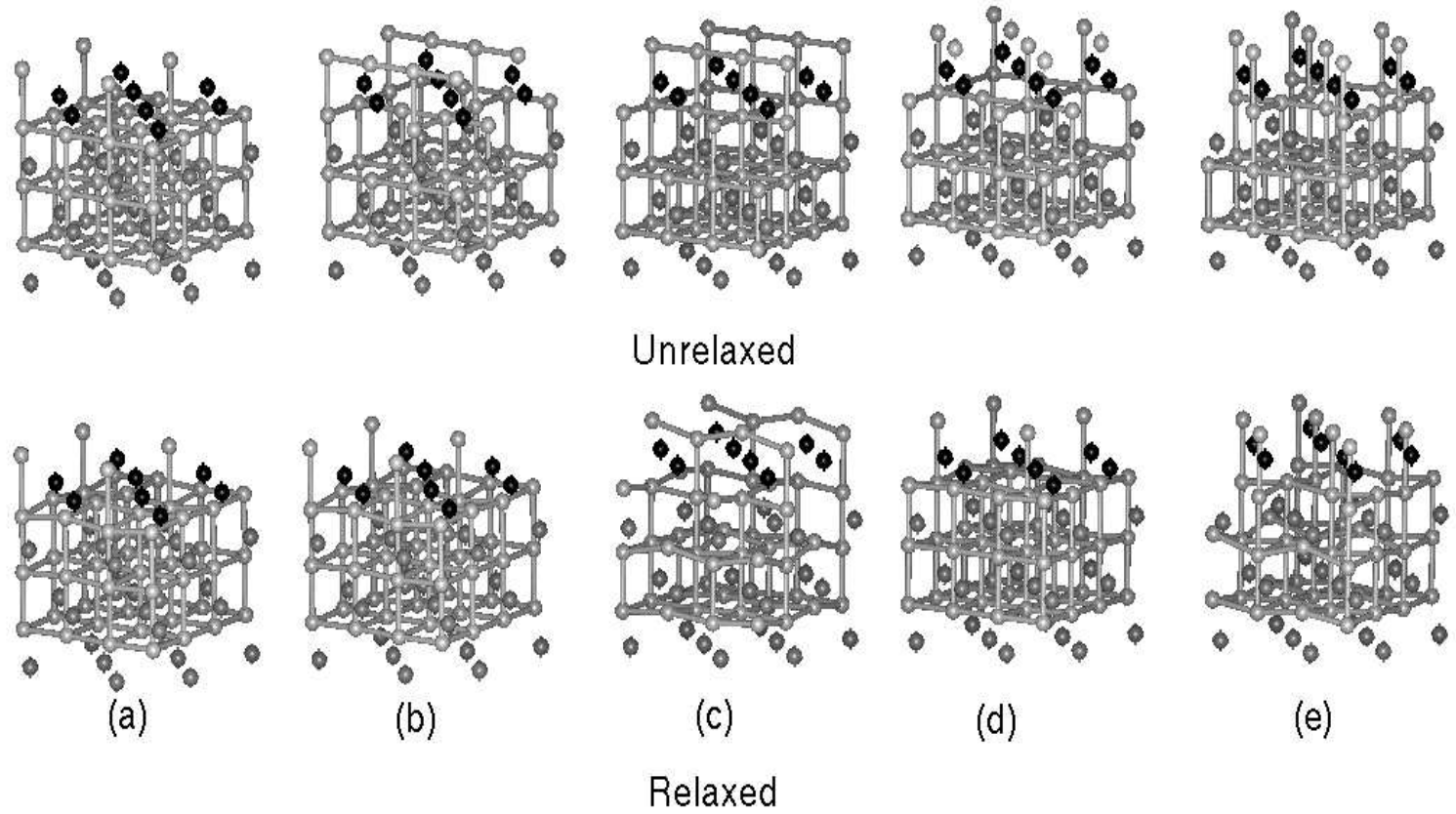


Figure 6.1: Defects on the (200) surface. The black atoms represent the polarons

Configuration	Energy (eV)		Z - Dipole	
	Unrelaxed	Relaxed	Unrelaxed	Relaxed
A	-3303.45	-3305.98	2.705	2.157
B	-3283.48	-3305.97	-2.705	2.157
C	-3279.76	-3300.63	-2.705	1.626
D	-3287.32	-3305.97	-2.705	2.157
E	-3285.91	-3302.39	-2.705	1.405

Table 6.2: Total energies for defects on the (200) surface

Configuration	Energy (eV)		Z - Dipole	
	Unrelaxed	Relaxed	Unrelaxed	Relaxed
A	-3284.36	-3296.01	1.562	0.428
B	-3287.80	-3294.68	1.562	0.70698

Table 6.3: Total energies for defects on the (111) surface

defect configurations are possible (Figure 6.2 and Table 6.3). Configuration A is the more stable of the two configurations, as the polarons are further apart. The vacancy relaxes downwards slightly into the plane below the surface as this position brings it closer to the polarons. The relaxation of layers tends to zero very rapidly (at about 5\AA), this is analogous to that seen for the relaxation of the perfect surfaces. Configuration B is less stable as the polarons are much closer together and hence repel each other more. The vacancy remains at its original position after relaxation as rearrangement to another position would not bring it any closer to the polarons.

6.3.3 The (220) surface

This is a type I surface. Thus for defect configuration in the same plane there is no dipole. Before relaxation the most stable configuration is that where both the polarons are at the surface and in the same plane as the vacancy (A in Figure 6.3, Table 6.4). However after relaxation, the energy difference between it and the other

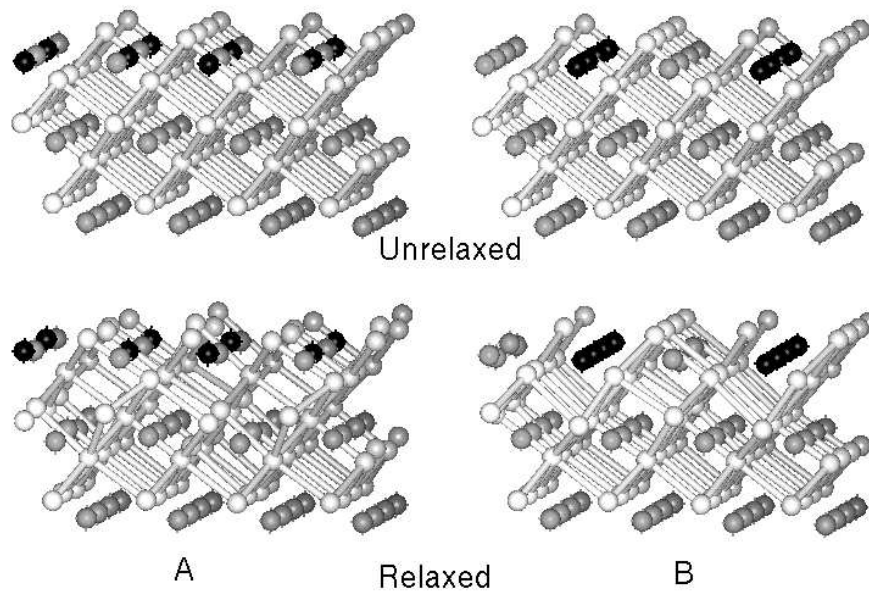


Figure 6.2: Defects on the (111) surface. The black atoms represent the polarons

Configuration	Energy (eV)		Z - Dipole	
	Unrelaxed	Relaxed	Unrelaxed	Relaxed
A	-3293.29	-3298.75	0.000	-0.207
B	-3287.88	-3298.48	1.913	-0.492
C	-3283.42	-3298.24	1.913	-0.436

Table 6.4: Total energies for defects on the (220) surface

configurations becomes much smaller, configuration A is only 0.4eV more stable than configuration B.

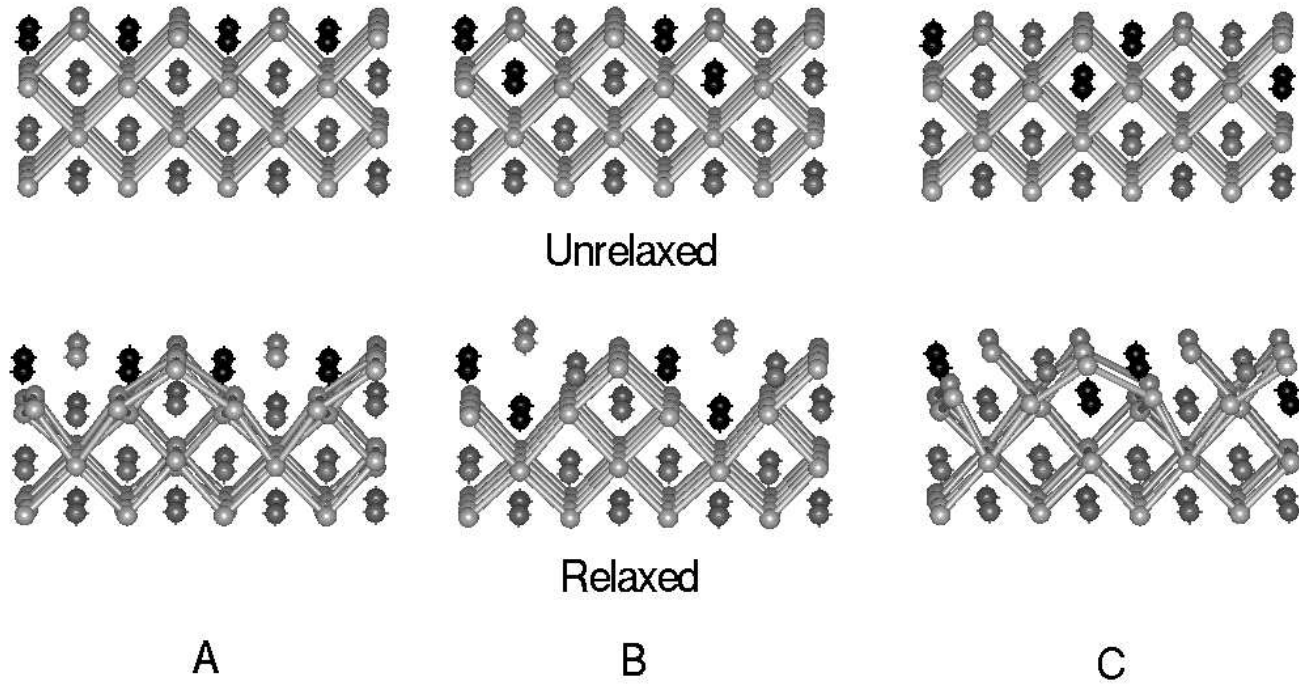


Figure 6.3: Defects on the (220) surface. The black atoms represent the polarons

6.3.4 The (331) surface

This face is stepped and hence contains many low coordinate ions. Thus it is highly probable that such a surface may be catalytically active. Figures 6.4 - 6.7 and Table 6.5 show the structure and energetics of the configurations investigated. Before relaxation the most stable of the configurations is that where the polarons are very close together but between the vacancy (Configuration A - Figure 6.4). On relaxation the situation changes, and the configuration becomes one of the least stable of the four configurations. In this configuration, during relaxation the vacancies move across from their corner sites to higher coordinate positions on the surface where they are more stable. After relaxation configuration B has the lowest total energy. Structurally, this is a result of the vacancy moving down into the plane below. This has the advantage of increasing its coordination but still keeping it close to the adjacent polaron. The position, also has the advantage of keeping the vacancy partially exposed to the surface. In fact a relaxation of the vacancy into the lower plane is seen in Configurations B, C, and D. Such behaviour seems to be the converse of that seen for the (200) surface where the configurations rearrange so that the vacancy is at the surface plane. No doubt, this is related to the polaron arrangements in configurations B - D which are similar in that the vacancy is initially placed between the polarons. This is not the case for Configuration A.

Configuration	Energy (eV)		Z - Dipole	
	Unrelaxed	Relaxed	Unrelaxed	Relaxed
A	-3711.68	-3727.52	0.6206	-1.2509
B	-3706.06	-3728.34	0.6206	-1.3176
C	-3709.36	-3728.08	1.862	1.3864
D	-3702.37	-3727.80	1.862	1.3602

Table 6.5: Total energies for defects on the (331) surface

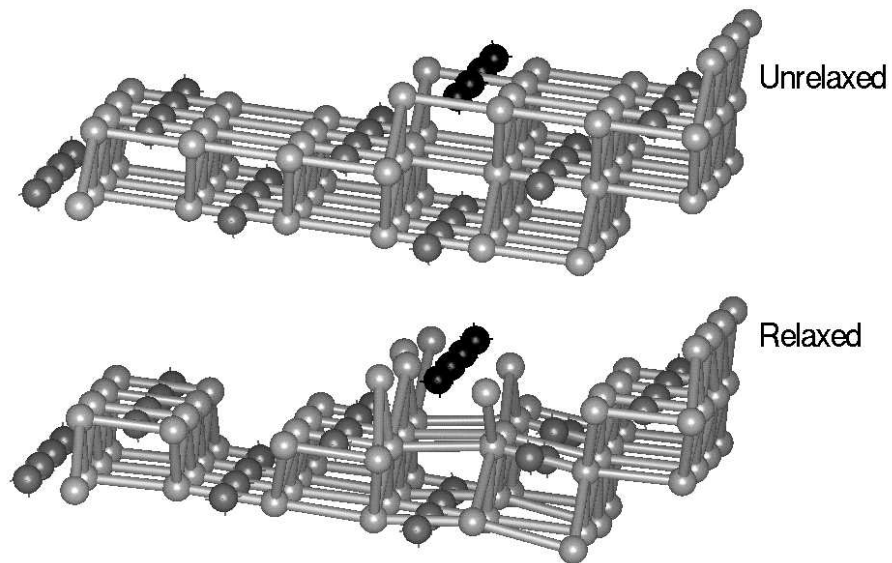


Figure 6.4: Defects on the (331) surface, Configuration A. The black atoms represent the polarons

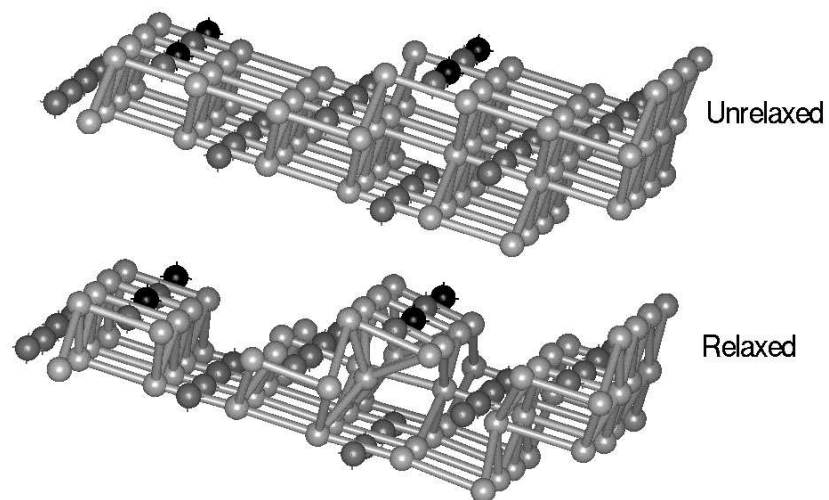


Figure 6.5: Defects on the (331) surface, Configuration B. The black atoms represent the polarons

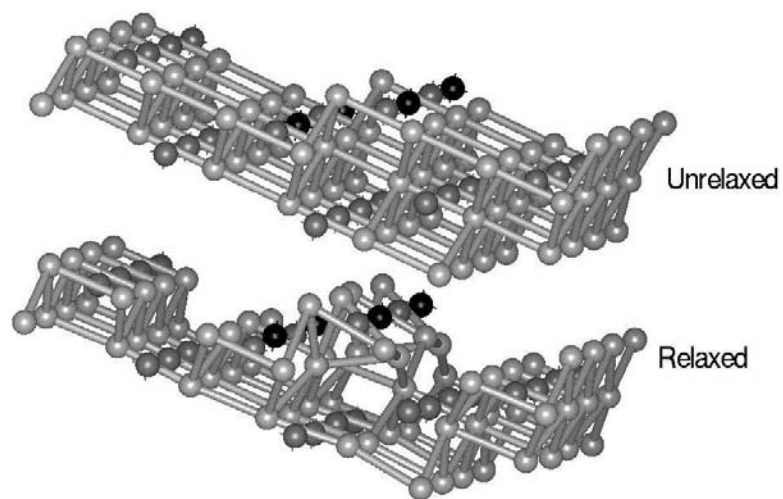


Figure 6.6: Defects on the (331) surface, Configuration C. The black atoms represent the polarons

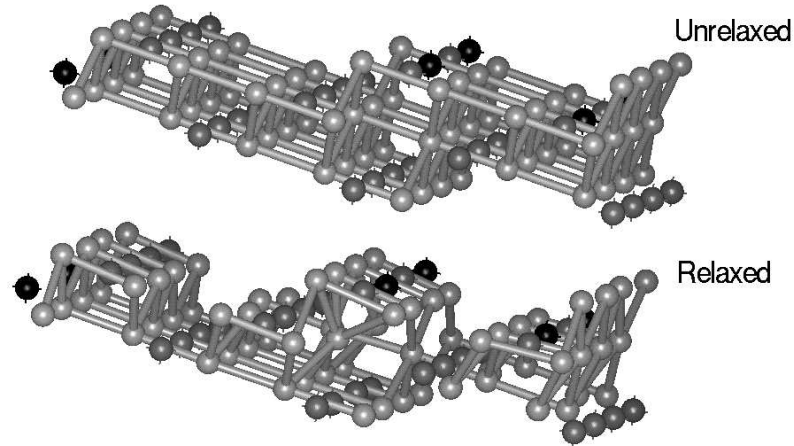


Figure 6.7: Defects on the (331) surface, Configuration D. The black atoms are the polarons

6.4 Defect formation energies

To determine the defect cluster formation energies on the surfaces, the energy of the most stable of the defect configurations were used, and the energy of the corresponding perfect surface subtracted. This enables us to compare the defect formation energies for different surfaces. The results are shown in Table 6.6. However, as there is one defect cluster per surface repeat unit the defect formation energies must be normalised to ensure a proper comparison; this is achieved by dividing the defect energy by the surface area. The results indicate that the (331) surface (Table 6.6) provides the lowest defect formation energy. However, this is not a definitive result as the repeat unit of this surface has the largest area. Consequently, this face will have the smallest defect - defect interactions, which can either lower or increase the defect formation energy. This belief is confirmed in Figure 6.8, which shows that the defect energy is

Surface	Defect energy (eV)	Surface Area (\AA^2)	Defect Energy per unit area ($\text{eV}\text{\AA}^{-2}$)
(111)	85.05	50.71	1.68
(200)	84.79	29.28	2.89
(220)	85.11	41.406	2.055
(331)	84.31	127.62	0.661

Table 6.6: The defect formation energy for the surfaces

proportional to the surface area, with the defect energy on the (200) surface being the highest. Undoubtly, a study similar to that in Chapter 4 would further our understanding of defects on the surface.

6.5 Summary

We have studied neutral defect clusters on several of the faces of ceria. The results indicate that the (200) surface rearranges such that it allows the oxygen vacancy to be at the surface. This converse is so for the (331) surface, here the vacancy prefers to be in a lower plane where it has a higher coordination. For both the (111) and (220) surfaces the orientations that give the smallest defect dipole are the most stable. Additionally, it has been shown that the defect-defect interactions must be considered when studying defect formation energies.

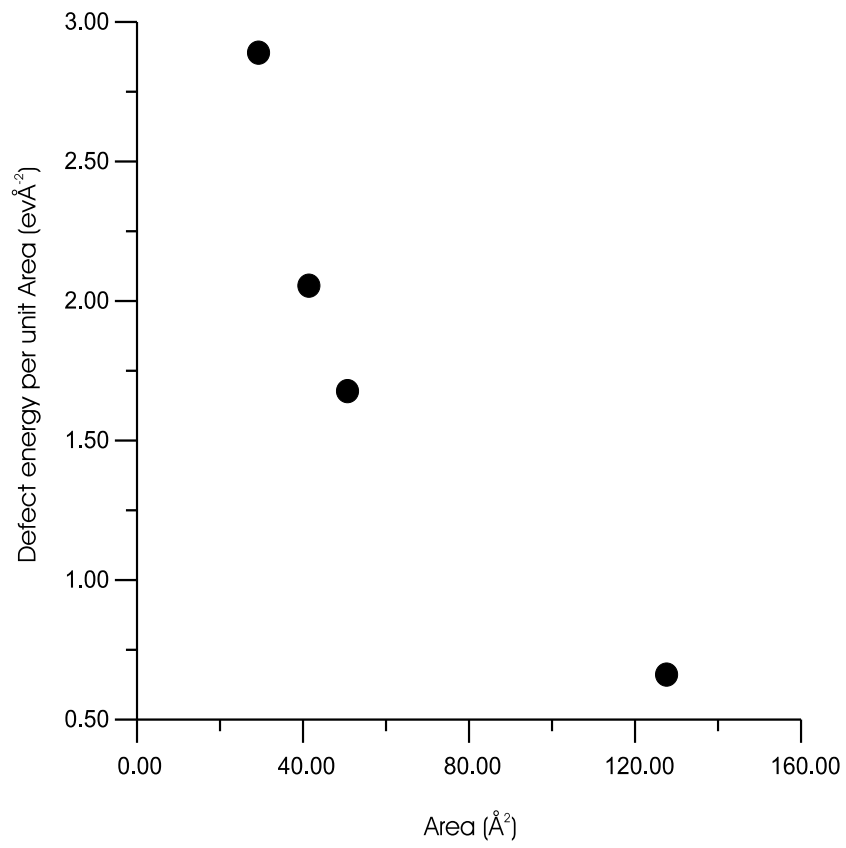


Figure 6.8: The normalised defect energy as a function of surface area